

Predicting failure stress for grain boundaries using average and local properties

S J Fensin, S M Valone, E K Cerreta and G T Gray III

Los Alamos National Laboratory, Los Alamos, New Mexico, 87545, USA

E-mail: saryuj@lanl.gov

Abstract: Several factors can affect the failure stress of a grain boundary, such as grain boundary structure, energy and excess volume, in addition to its interactions with dislocations. In this paper, we focus on the influence of grain boundary energy, excess volume and plasticity at the boundary on the failure stress of a grain boundary, in copper from molecular-dynamics simulations. Flyer plate simulations were carried out for four boundary types with different energies and excess volumes. These boundaries were chosen as model systems to represent various boundaries observed in “real” materials. Simulations indicate that there is no direct correlation between the void nucleation stress of a boundary and either its energy and excess volume. This result suggests that average properties of grain boundaries alone are not sufficient indicators of the failure strength of a boundary. However, local boundary properties related to the ability of a grain boundary to undergo plastic deformation are better markers of its strength.

1. Introduction

Research over the past few decades has provided a wealth of data regarding the influence of microstructure on damage nucleation and evolution during plate-impact experiments. Microstructural features such as grain boundaries, inclusions, vacancies and heterogeneities can promote plastic deformation and affect the response of a material to dynamic loading [1-7]. In particular, grain boundaries can be important nucleation sites for defects that eventually lead to failure. One specific failure process, spall, that is shock compression-and-release-induced fracture of solids, motivates this investigation. Grain boundaries in metals have their own structure, distinct from regions of perfect crystalline material. Not surprisingly then, individual grain boundaries with varying structures can have unique responses under plate impact experiments. In fact, observations of spall failure in high-purity Cu metal demonstrate, that not only does spall occur preferentially at grain boundaries [8] but also certain special boundaries are more resistant to spall [9]. This point is also supported by work of Wayne *et al.* [10] who found that grain boundaries *with certain misorientations*, in polycrystalline Cu, are preferred locations for intergranular damage. The fact that these voids generated by voids tend to be localized at specific grain boundaries, suggests that the standard geometric descriptors of dislocation-based mechanisms cannot explain the reduced propensity of failure at special CSL boundaries [8,11]. This statistical analysis indicates the importance of the GB structure and its association with the deformation behaviour. During dynamic loading, this sort of localization of voids at specific grain boundaries based on the boundary structure is often ignored in continuum and hydrodynamic models of spall failure since it is not well understood. This paper attempts to correlate susceptibility of a boundary to failure to its average and local properties in the hope that it would also shed light on possible mechanisms for void nucleation.



2. Simulation Methodology

2.1 Grain Boundaries

In order to separate the effects of grain boundary energy (GBE) and excess volume (EV) from other average properties of the boundaries, four boundaries were chosen -- representing a range in these GB properties encountered in “real” polycrystalline materials. We performed shock simulations at 300 K, in a flyer-plate geometry, on the following four different grain boundaries in Cu:

- $\Sigma 11$ $\langle 101 \rangle$ $\{545\}$ - $\{181\}$ 50.48° asymmetric tilt
- $\Sigma 11$ $\langle 101 \rangle$ $\{545\}$ - $\{181\}$ 50.48° asymmetric tilt boundary whose structure was disordered by annealing and subsequently quenching the $\Sigma 11$ asymmetric tilt boundary
- $\Sigma 5$ $\langle 100 \rangle$ $\{310\}$ 36.9° symmetric tilt
- $\Sigma 3$ $\langle 110 \rangle$ $\{112\}$ 36.9° symmetric tilt

The relaxed structures and properties for these boundaries at 0 K are shown in figure 1 and table 1.

The range of grain boundary energies and excess volumes, shown in table 1, match well with values calculated in previous works [12-14]. It is interesting to note that only changing the local structure of the $\Sigma 11$ grain boundaries, even though the orientation relationship between the two grains is the same, resulted in a 14% and 97% change in GBE and EV, respectively. Even though the $\Sigma 5$ boundary is a symmetric tilt boundary, it is the highest energy boundary studied in this paper because it is a $\langle 100 \rangle$ -tilt boundary. In general, for the same Σ value, the energy of $\langle 100 \rangle$ tilt boundaries is higher than the $\langle 110 \rangle$ boundaries [15]. The $\Sigma 3$ incoherent twin boundary is the lowest energy boundary studied here and corresponds to the low energy structure for the incoherent twin boundary as discussed in [13].

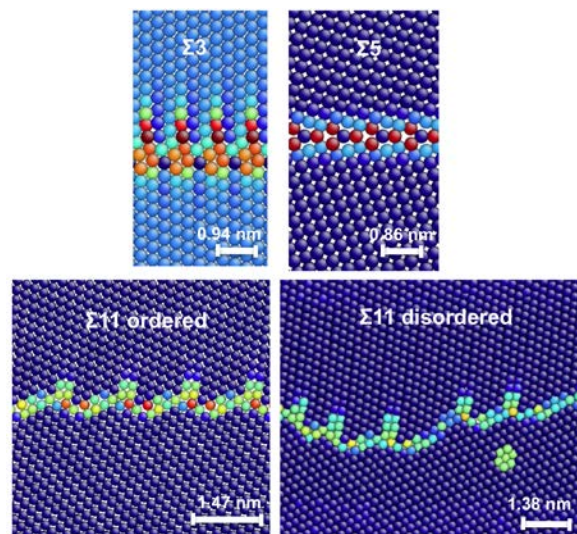


Figure 1: Relaxed GB structures for the four boundaries used in this study. The atoms are colored by the centrosymmetry [16] parameter where blue represents atoms close to an fcc environment and red represents atoms not in fcc configuration any more. The range of the centrosymmetry parameter in all the images is different in order to highlight the GB. Reproduced with permission from reference [17].

2.2 Plate-Impact Simulations:

All the MD simulations were based on an embedded-atom method (EAM) interatomic potential model for copper developed by Mishin *et al.* [18]. Our MD simulations used a combination of SOLVER [19-22] for initially relaxing the grain boundaries at 0 K and LAMMPS [23] for finite temperature and shock-loading simulations. The details of the LAMMPS shock simulations are discussed in [17]

2.3 Post-Impact Analysis:

To track the shock wave and other physical properties during the shock simulation, the simulation cell is divided into bins of size 0.55 nm in width along the shock direction and the average physical properties such as particle velocity and stresses are obtained within each bin. The void nucleation stress for the boundaries was calculated from the peak stress in the profiles immediately before void nucleation, in the shock direction. The energy and excess volume of the grain boundary was computed as the total energy/volume of the unconstrained atoms, less the bulk crystal energy/volume for the same number of atoms, divided by the planar area of the boundary from the relaxed grain boundary structures at 0K.

Table 1: The grain-boundary types used in the MD simulations along grain boundary energy and excess volume at 0 K. ST, AT and ICT refer to symmetric tilt, asymmetric tilt and incoherent twin boundaries, respectively. Reproduced with permission from reference [17].

GB type	γ_{GB}^o (J/m ²)	V_{Excess} (nm ³ /nm ²)
$\Sigma 11 \langle 101 \rangle \{545\} - \{181\} 50.48^\circ$ AT	0.667	0.021
$\Sigma 11 \langle 101 \rangle \{545\} - \{181\} 50.48^\circ$ disordered AT	0.775	0.807
$\Sigma 5 \langle 100 \rangle \{310\} 36.9^\circ$ ST	0.913	0.054
$\Sigma 3 \langle 110 \rangle \{112\} 36.9^\circ$ ICT	0.592	0.021

3. Results and Discussion

Spall is a type of fracture and hence the effect of grain boundary energy on spall can be studied by using the following equation [24]:

$$\gamma_f = 2\gamma_s - \gamma_{GB} + \gamma_p, \quad (1)$$

where γ_f , γ_s , γ_{GB} and γ_p are the fracture energy, free surface energy, the grain boundary energy and the plastic work associated with intergranular fracture, respectively. Thus, in addition to γ_{GB} , we also investigated γ_s as another possible factor that can affect the correlation between GBE and the fracture strength of a material. Our study shows that there was an insignificant difference in γ_s amongst the four boundaries. These results are in line with reference [25] where the authors did not notice a significant change in surface free energy with orientation. We can also combine the terms $2\gamma_s$ and γ_{GB} into the work of separation, $W_{sep} = 2\gamma_s - \gamma_{GB}$ [26], which is defined as the ideal reversible work required to separate an interface into two free surfaces. It is important to note that, even though W_{sep} does not take into account the plastic and elastic properties of the material along with other factors that can be important in predicting the strength of a material, it is an integral interfacial property that can be used to predict the upper bound on the theoretical fracture strength of an interface.

Figure 2 shows plots of GBE, EV and W_{sep} vs. void nucleation stress for the four boundaries selected for this study. It is clear from this plot that there is no direct correlation between grain boundary energy, excess volume, work of separation and void nucleation stress. In fact, the void nucleation stress for the $\Sigma 11$ ordered and the $\Sigma 5$ boundary is about the same, even though their energies are different. Similar observations were made for the excess volume, in spite of the much greater range of values sampled. For instance, even though the excess volume for the disordered $\Sigma 11$ boundary is much higher than that of the other boundaries, its void nucleation stress lies between that of $\Sigma 3$ and $\Sigma 11$ ordered boundaries. Nor was any correlation found between the void nucleation stress of a GB and its Σ number. Further no correlation was found between W_{sep} and the void nucleation stress as expected given that γ_s was similar for all the boundaries. Even though the difference in W_{sep} for the $\Sigma 5$ and $\Sigma 11$ ordered boundaries is 0.15 J/m², their void nucleation stresses were found to be nearly the same. These results suggest that γ_s , γ_{GB} and hence W_{sep} are not playing a significant role in determining the fracture strength of these boundaries. Furthermore, it suggests that the average properties do not capture the mechanisms for void nucleation at grain boundaries in Cu.

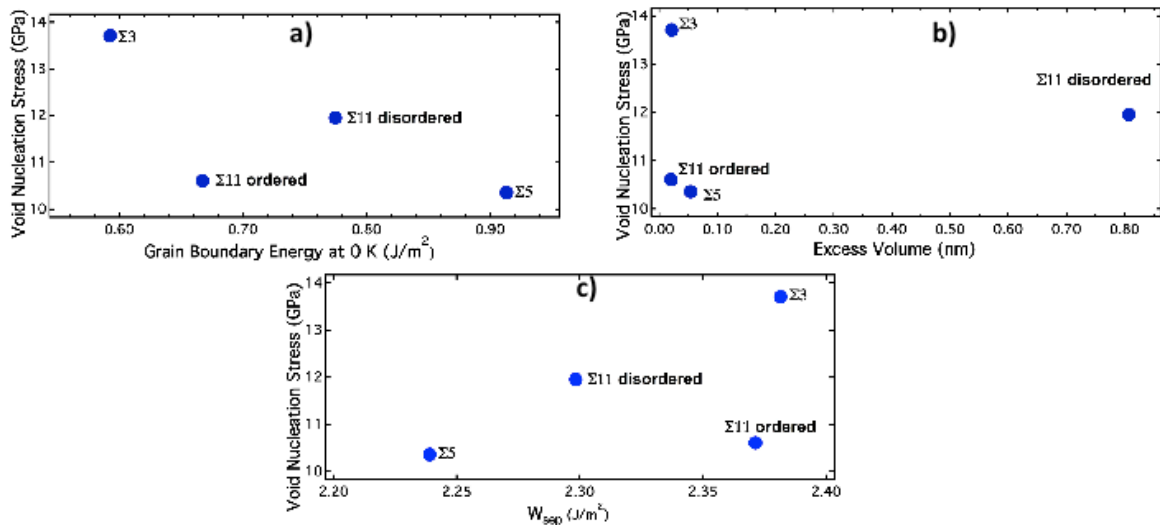


Figure 2: Plots of void nucleation stress vs. a) grain boundary energy, b) excess volume and c) work of separation for the four boundaries used in this study. Reproduced with permission from reference [17].

These results suggest that the plastic work term, γ_p , could be determinant of the fracture strength of an interface in ductile materials. In the case of brittle materials, in γ_p equation (1) is low, and hence GBE can dominate the fracture energy and hence the fracture strength of a material. This explains the role of grain boundary energy in molybdenum, a classically brittle metal, where Tsurekawa *et al.* [27] did observe a correlation between fracture strength of a boundary and GBE. However, this analysis is more complicated in the case of ductile materials where γ_p can be significant. In ductile materials, especially under dynamic damage conditions, extensive plastic work precedes and then competes with failure processes [9,10].

Hence, if the magnitude of γ_p is large, it may dictate the void nucleation stress of a material instead of the GBE. This point is further emphasized by the results for the two $\Sigma 11$ boundaries where even though the orientation in the two grains was held constant, the void nucleation stresses of the boundaries differed by 1.34 GPa or 11.2%. This difference was attributed to the fact that the $\Sigma 11$ ordered boundary did not undergo any plastic deformation under shock compression whereas the disordered boundary emitted Shockley partials from the boundary [28]. In this case, plastic deformation at the boundary due to dislocation emission under shock compression, was acting as a dissipation mechanism for the applied stress. Hence higher plastic deformation during shock compression retarded void nucleation by dissipating some of the applied stress. These results demonstrate that GBE and EV may not always be the most critical factors controlling damage at a boundary and perhaps local properties such as the ability of a boundary to plastically deform needs to be taken into account.

4. Summary

In this study, we probed four different grain boundaries, using MD simulations, in order to quantify any correlations between the void nucleation stress at a GB and grain boundary energy, excess volume, and work of separation. The boundaries were chosen such that they had varying structures, 0 K energies and excess volumes. The results of plate-impact simulations at a particle velocity of 0.5 km/s show that there is *no discernible correlation* between the void nucleation stress and GB energy, excess free volume and work of separation. The phenomena involved in damage are complex and involve many competing processes. GBE and EV individually fail to predict these complex phenomena in the cases investigated here. Local heterogeneities within a GB, such as ledges, inclusions, and high-energy atoms, affect its ability to dissipate stress, and may be the determinants of failure strength in the cases considered here. In fact, results from the $\Sigma 11$ boundaries qualitatively suggest that perhaps a boundary's ability to plastically deform under shock compression, prior to void nucleation, is an important

dissipation mechanism for the applied stress. The idea of failure strength as a competition among various stress dissipation processes at grain boundaries is necessary to understand and control the failure process.

Acknowledgements

Los Alamos National Laboratory is operated by LANS, LLC, for the NNSA and the U.S Department of Energy under contract DE-AC52-06NA25396. This work has been supported by the office of Basic Energy Sciences and the Energy Frontier Research Center of Materials at irradiation and mechanical extremes (CMIME), as well as the DOD/DOE Joint Munitions Program, Advanced Simulation and Computing program and LDRD-DR 20100026. SJF and SMV also want to acknowledge helpful discussions with R. G. Hoagland.

References

- [1] Curran D R, Seaman L and Shockley D A 1987 *Phys. Rep.* **147** 370-1573
- [2] Seaman L, Curran D R and Shockley D A 1976 *J. Appl. Phys.* **47** 4814-26
- [3] Meyers M A and Aime C T 1983 *Prog. Mater. Sci.* **28** 1
- [4] Curran D R, Seaman L and Shockley D A 1977 *Phys. Today* **30** 46-55
- [5] Minich R W, Cazamias J, Kumar M and Schwartz A 2004 *Met. and Mat. Trans. A* **35** 2663-73
- [6] Minich R W, Kumar M, Schwartz A and Cazamias J 2006 *AIP Conf. Proc.* **845** 642-5
- [7] Gray III G T 2012 *Ann. Rev. Mater. Res.* **42** 285-303
- [8] Kanel G I, Rasorenov S V, and Fortov V E 1992 *Shock wave and high-strain-rate phenomena in materials*, ed M A Meyers *et al.* (New York, NY: Marcel Dekker) 775
- [9] Escobedo-Diaz J P, Dennis-Koller D, Cerreta E K, Patterson B M, Bronkhorst C A, Hansen B L, Tonks D and Lebensohn R A 2011 *J. Appl. Phys.* **110** 033513
- [10] Wayne L, Krishnan K, DiGiacomo S, Kovvali N, Peralta P, Luo S N, Greenfield S, Byler D, Paisley D, McClellan K J, Koskelo A and Dickerson R 2010 *Scripta Mater.* **63** 1065-8
- [11] Cerreta E K, Escobedo-Diaz J P, Perez-Bergquist A, Koller D, Trujillo C P, Gray III G T, Brandl C and Germann T C 2012 *Scripta Mater.* **66** 638-41
- [12] Schmidt C, Finnis M W, Ernst F and Vitek V 1998 *Phil. Mag. A* **77** 1161
- [13] Wang J, Anderoglu O, Hirth J P, Misra A and Zhang X 2009 *App. Phys. Lett.* **95** 021908
- [14] Olmsted D L, Foiles S M and Holm E A 2009 *Acta Mater.* **57** 3694
- [15] Sangid M D, Ezaz T, Sehitoglu H and Robertson I M 2011 *Acta Mater.* **59** 283
- [16] Kelchner C L, Plimpton S J and Hamilton J C 1998 *Phys. Rev. B* **58** 11085
- [17] Fensin S J, Valone S M, Cerreta E K and Gray III G T 2012 *J. Appl. Phys.* **112** 083529
- [18] Mishin Y, Mehl M J, Papaconstantopoulos D A, Voter A F and Kress J D 2001 *Phys. Rev. B* **63** 224106
- [19] Hoagland R G, Daw M S and Hirth J P 1991 *J. Mater. Res.* **6** 2565
- [20] Demkowicz M J, Wang J and Hoagland R G 2008 *Interfaces between dissimilar crystalline solids in Dislocations in Solids*, **14**: A Tribute to F. R. N. Nabarro, ed. by J. P. Hirth (Amsterdam: Elsevier) 141-206
- [21] Henager C H, Kurtz R J and Hoagland R G 2004 *Philos. Mag.* **84** 2277-2303
- [22] Hoagland R G, Kurtz R J and Henager C H 2004 *Scripta Mater.* **50** 775-779
- [23] Plimpton S J 1995 *J. Comp. Phys.* **117** 1-19
- [24] Watanabe T and Tsurekawa S 2005 *Mater. Sci. Forum* **482** 55-62
- [25] Liu C L, Cohen J M, Adams J B and Voter A F 1991 *Surf. Sci.* **253** 334-44
- [26] Finnis M W 1996 *J. Phys. Condens. Matter* **8** 5811-36
- [27] Tsurekawa S, Tanaka T and Yoshinaga H 1994 *Mater. Sci. Eng.* **A176** 341-8
- [28] Fensin S J, Valone S M, Cerreta E K, Escobedo-Diaz J P, Gray III G T, Kang K and Wang J 2012 *Model. Simul. Mater. Sc.* **21** 150